PHYSICAL REVIEW C VOLUME 35, NUMBER 1 JANUARY 1987

Production and decay of highly excited nuclear systems formed in ^{84}Kr + ^{12}C and ^{27}Al collisions at 35 MeV/nucleon

F. Auger,[a] B. Berthier,[a] A. Cunsolo,[b] A. Foti,[b],[c] W. Mittig,[c] J. M. Pascaud,[d] E. Plagnol,[e] J. Québert,[d] and J. P. Wieleczko[a]

[a] *Département de Physique Nucléaire, Basse Energie, Centre d'Etudes Nucléaires, Saclay, 91191 Gif-sur-Yvette, Cédex, France*

[b] *Dipartimento di Fisica and Istituto Nazionale di Fisica Nucleare, I-95129 Catania, Italie*

[c] *GANIL, 14021 Caen Cédex, France*

[d] *Centre d'Etudes Nucléaires Le Haut Vigneau, 33170 Gradignan, France*

[e] *Institut de Physique Nucléaire, 91406 Orsay Cédex, France*

(Received 28 January 1986)

Masses, atomic numbers, and energies of heavy ($M \geq 15$ nucleons) particles emitted in the reactions induced by ^{84}Kr on ^{12}C and ^{27}Al at 35 MeV/nucleon have been measured by means of two time-of-flight silicon counter telescopes. Experimental results from single and coincidence measurements are presented and discussed in the framework of the statistical sequential decay model following complete and incomplete fusion in the entrance channel.

I. INTRODUCTION

The behavior of nuclear matter at very high excitation energy has raised recently considerable interest from both experimental[1–3] and theoretical[4,5] points of view. New phenomena, such as heavy fragment emission,[6] multifragmentation, and phase transitions,[7] are expected to show up with significant cross sections below the explosion limit.[8]

To investigate this domain, the study of residues of the central collisions emitted in heavy ion reactions induced at intermediate energies ($10 \leq E_{\text{lab}} \leq 100$ MeV/nucleon) should be the appropriate experimental tool.

However, projectile and target fragmentation is a dominant process in this energy range,[9,10] and it may hide the presence of an equilibrated and very hot nuclear system. In order to favor the formation and observation of such systems, we studied, using inverse kinematics, the very asymmetric ^{84}Kr + ^{12}C and ^{84}Kr + ^{27}Al reactions at 35 MeV/nucleon, in which the equilibration of the involved composite nuclei is expected to be rapid. In Ref. 11 it is shown that the potential energy decreases steeply for increasing asymmetry, for l values up to about $60\hbar$, and thus a strong driving force for the absorption of the smaller partner by the larger one will result. Due to this choice, the yield of intermediate mass nuclei should contain very small contributions from quasielastic processes.

The experimental methods and results are presented in Sec. II, together with the analysis of the peculiar kinematics of the fragments with masses in the range $20 \leq M \leq 60$.

In Sec. III we deal with the theoretical analysis done in order to achieve a quantitative understanding of the heavy fragment yields. Following the approach of Moretto[12] and Swiatecki,[13] the statistical model predictions for the emission of heavy fragments from a hot composite system have been compared to the experimental data. Conclusions are drawn in Sec. IV. Some partial results have been published elsewhere.[3,14,15]

II. EXPERIMENTAL METHODS AND RESULTS

The 2.94 GeV ^{84}Kr beam of 10—50 (electric) nA ($\sim 10^{10}$ particles/s) intensity, delivered by the GANIL accelerator at Caen (France), was used to bombard 0.4 mg/cm^2 ^{12}C and 1.5 mg/cm^2 ^{27}Al targets. It is important to note that in inverse kinematics experiments the reaction products have high velocities and are focused at forward angles. The first feature avoids threshold effects even for the heaviest products; the second permits the extraction of total cross sections from the measurement of angular distributions in a narrow angular range and allows a good efficiency in coincidence measurements.

In the present experiment two time of flight telescopes, each consisting of three solid state detectors (50, 100, and 4000 μm), were used to detect the reaction products. Start and stop detectors were located, respectively, 1 and 2.4 m from the target. The time resolution [full width at half maximum (FWHM) of 130 ps] permitted the separation of masses up to $M \sim 50$ and the ΔE-E identification resolved all observed atomic numbers. One telescope (A) measured angular distributions from 1.75° to 14°, i.e., well above the grazing angles,[16] while the other (B) was kept at 3° on the other side of the beam for coincidence measurements. Absolute values of the cross sections were obtained from known target thickness, solid angle (0.036 msr), and integrated beam current with an estimated uncertainty of $\sim 20\%$.

Figure 1 shows typical velocity versus atomic number plots of particles detected at 5° for carbon and aluminum targets, while the velocity versus mass plots for several detection angles are shown in Fig. 2. Typical velocity spectra as a function of detection angles and of fragment masses (integrated over five mass units) are displayed in Fig. 3. In these figures one clearly observes at forward angles a relevant yield of projectile-like fragments mainly due to quasielastic and fragmentation processes. In contrast, the intermediate mass fragments show twofold velocity distributions and cover an increasing angular domain with decreasing mass. In the low velocity branch of the light nuclei there is probably some contribution of quasielastic and fragmentation processes involving the target.

The evolution of the two components with detection angle and mass suggests that the reaction products originate from the splitting of a composite system. The low and high velocity components correspond, respectively, to backward and forward emission of the observed fragment with respect to the center of mass of the moving emitter. Simple binary kinematical calculations support this picture.

In fact, we have

$$V = V_{\mathrm{em}}\cos\theta \pm (V_{\mathrm{c.m.}}^2 - V_{\mathrm{em}}^2 \sin^2\theta)^{1/2} , \qquad (1)$$

where V is the laboratory velocity of the detected fragment of mass M, $\mathbf{V}_{\mathrm{c.m.}}$ its velocity in the emitter frame, $\mathbf{V}_{\mathrm{em}}$ is the laboratory velocity of the decaying composite system, and θ is the detection angle. This relation is strictly valid for a two body reaction. However, light particle evaporation, independent of whether it takes place before or after the emission of a heavy fragment, mainly broadens the observed distributions and changes very little their mean values. $V_{\mathrm{c.m.}}$ and V_{em} are obtained from the experimental centroids of the two velocity components using Eq. (1). The results are shown in Fig. 4 for several angles θ as a function of the residual mass.

The upper part [Fig. 4(a)] shows the velocity of the emitter V_{em} obtained in this way. In the case of the carbon target, the experimental value of V_{em} corresponds essen-

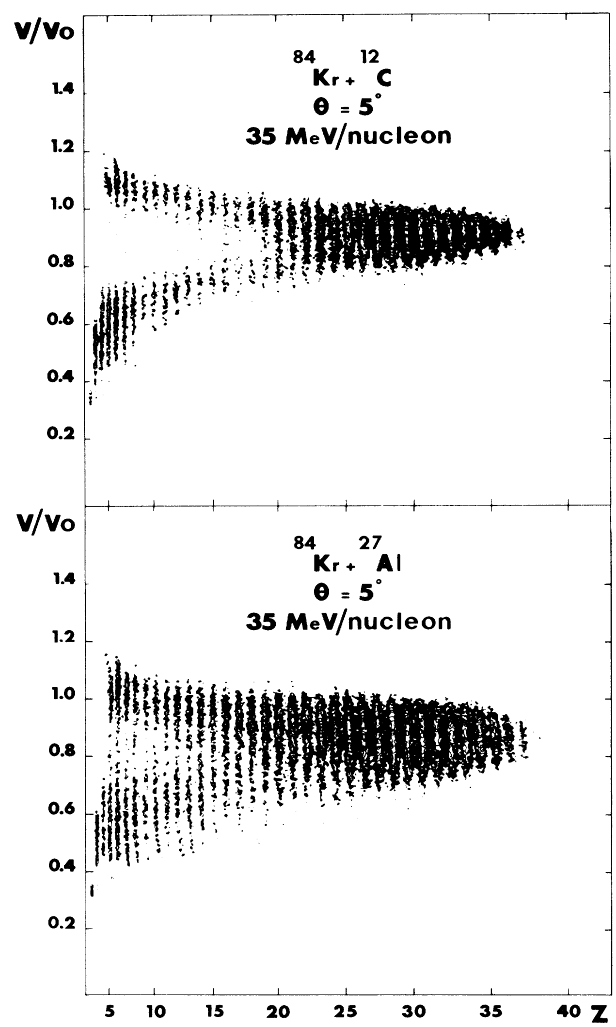

FIG. 1. Two-dimensional velocity vs atomic number spectra for heavy residues detected at $\theta = 5°$ in the ^{84}Kr+^{12}C and ^{84}Kr+^{27}Al reactions at 35 MeV/nucleon. V_0 is the projectile velocity.

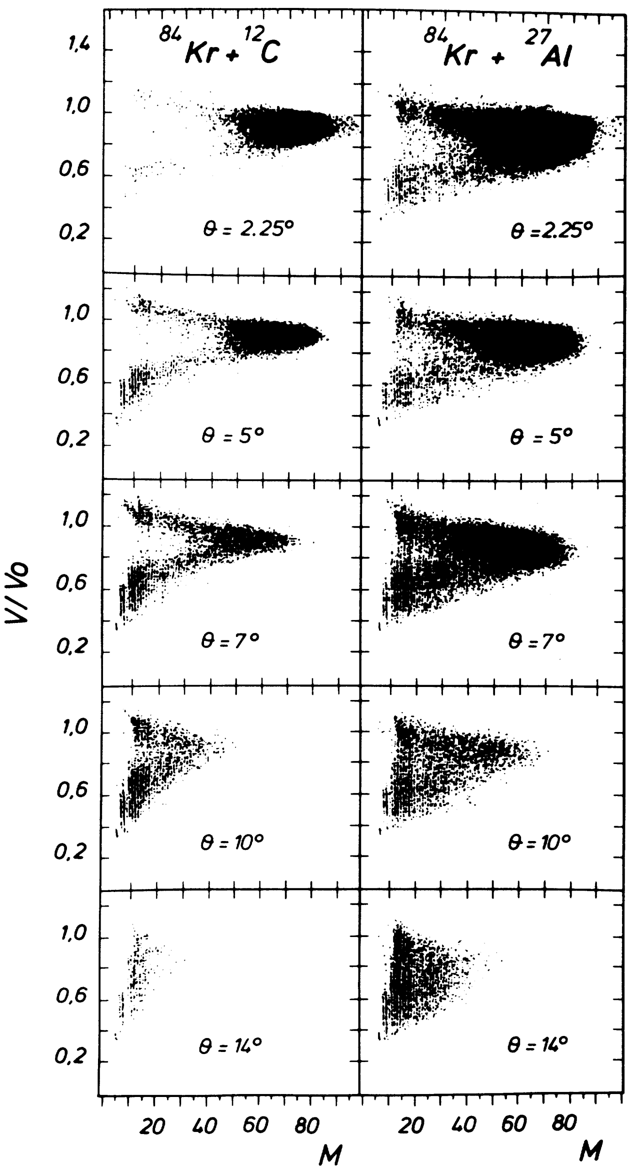

FIG. 2. Two-dimensional velocity vs mass spectra observed at several angles.

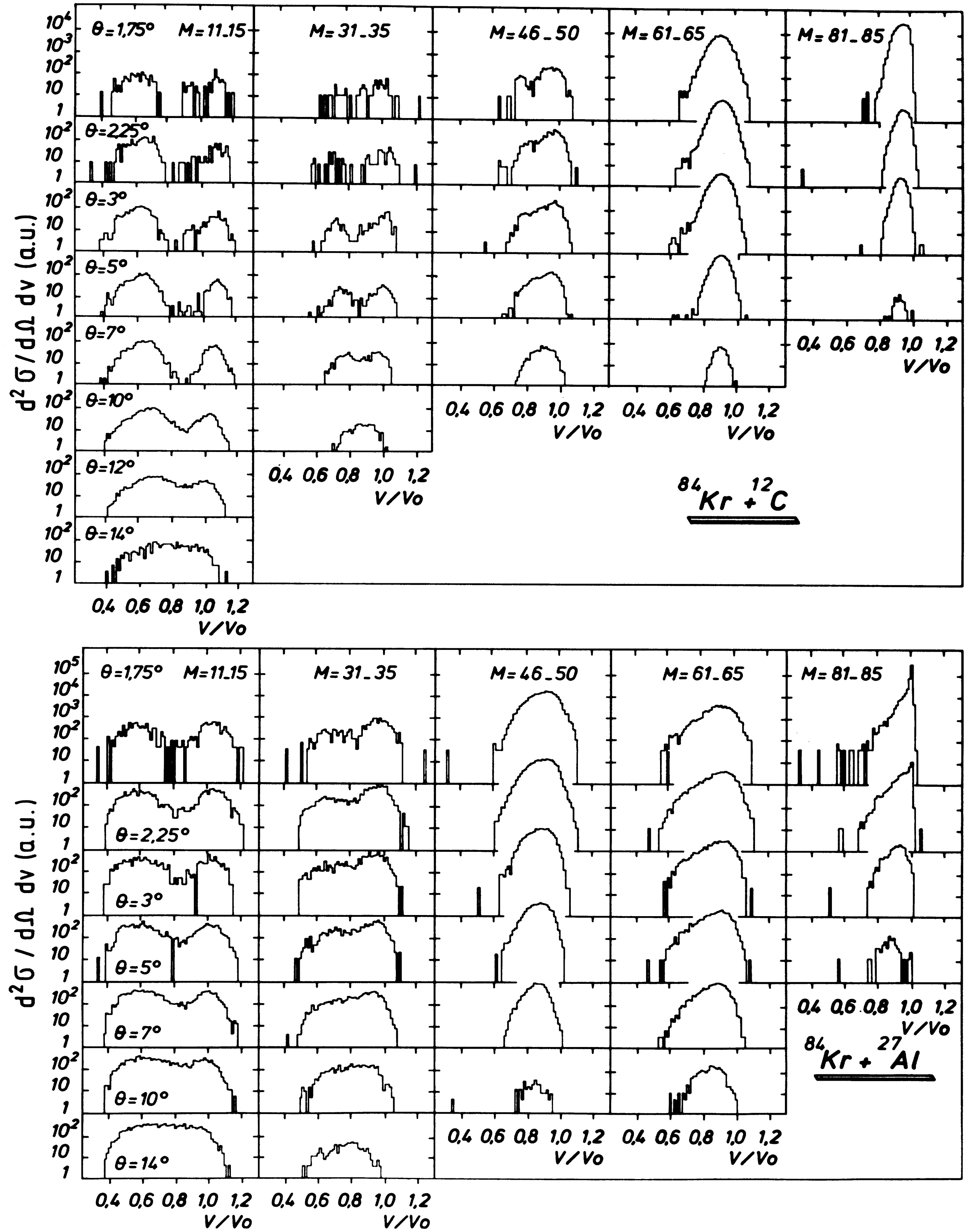

FIG. 3. Velocity spectra as a function of mass at different angles.

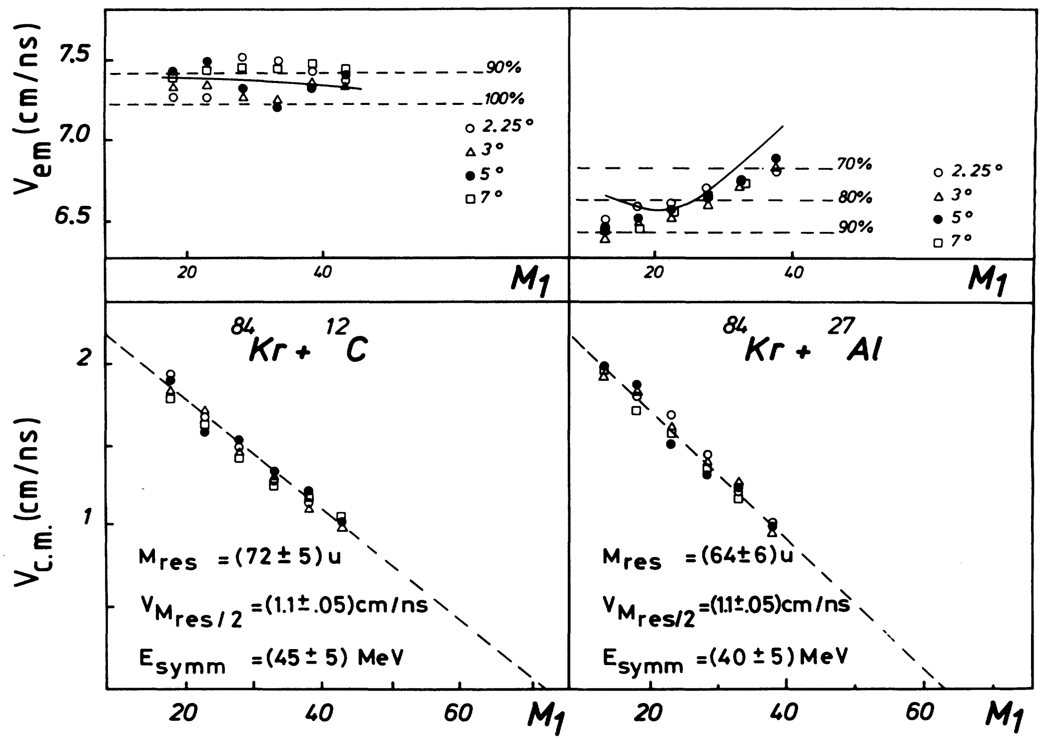

FIG. 4. Upper part: emitter velocities vs mass extracted from data at several detection angles using Eq. (1) (see text). The dashed lines indicate the velocity values corresponding to the indicated values of linear momentum transfer in inverse kinematics. The solid line is the prediction of the model of the geometrical incomplete fusion process followed by statistical emission of the hot heavy fragments discussed in Sec. III. Lower part: velocity in the emitter frame of the reaction products as a function of the mass. The dashed lines represent the linear behavior predicted from Eq. (2).

tially to complete momentum transfer. For aluminum we find 70–90 % momentum transfer, strongly depending on the detected mass.

The value obtained for Kr + C is higher than expected from the Viola systematics for linear momentum transfer.[17] However, the experimental value given here corresponds to the mean momentum transfer that leads to emission of intermediate mass fragments ($M=15$–40) and may differ from the systematics of Viola that corresponds to the overall mean value. The fact that the value observed here is higher than the systematics indicates that most central collisions are selected by the exit channels studied here. The experimental results are well reproduced by the geometrical incomplete fusion model discussed in Sec. III, as shown by the solid lines in Fig. 4.

The lower part [Fig. 4(b)] shows that $V_{\mathrm{c.m.}}$ depends linearly on the fragment mass. This is expected from the binary disintegration kinematics. Consider that M_1 and M_2 are the masses of the two fragments with $M_1+M_2=M_{\mathrm{res}}$ having the kinetic energies E_1 and E_2 related to a symmetric disintegration via the relation[16,18]

$$E_1+E_2=4E_{\mathrm{sym}}M_1M_2/(M_1+M_2)^2 \ .$$

Energy and linear momentum conservation lead to

TABLE I. Linear momentum transfer (LMT), mass transfer (ΔM), excitation energy (E^*), ϵ, residual mass (M_{res}) obtained by different methods, and the kinetic energy of fissionlike products for the two systems studied.

System	^{84}Kr+^{12}C	^{84}Kr+^{27}Al
LMT^{a} (%)	95 ±10	(70–90)±10^{b}
ΔM^{c}	11.6	21.6
E^* (MeV)	357 ±40	600 ±60
ϵ^{d} (MeV/nucleon)	3.7±0.4	5.7 ±0.5
$M_{\mathrm{res}}{}^{a}$	72 ±5	64 ±6
$M_{\mathrm{res}}{}^{e}$	77 ±4	71 ±7
$M_{\mathrm{res}}{}^{f}$	76	70
$E_{\mathrm{sym}}{}^{a}$ (MeV)	45 ±5	40 ±5

[a]From singles using Eqs. (1) and (2) (see Fig. 4); LMT is the linear momentum transfer in inverse kinematics.
[b]The value depends on the ejectile mass (see Fig. 4).
[c]Using $\Delta M=M_{\mathrm{target}}\times\mathrm{LMT}$.
[d]Using $E^*=84\Delta M\times 35$ MeV/$(84+\Delta M)$ and $\epsilon=E^*/(84+\Delta M)$.
[e]From coincidence measurements (see Fig. 9); the quoted error corresponds to the experimentally observed half-width at half maximum.
[f]From the minimum observed in the mass yield.

$$V_{\mathrm{c.m.}} = \frac{M_{\mathrm{res}} - M_1}{M_{\mathrm{res}}} \left[8 \frac{E_{\mathrm{sym}}}{M_{\mathrm{res}}} \right]^{1/2} . \tag{2}$$

The values reported in Table I are obtained using Eq. (2) and Fig. 4. Relation (2) may be not strictly valid for the aluminum case because of the mass dependence of the momentum transfer. The resulting E_{sym} values correspond closely to the one of the Viola systematics[18] of separation energies for symmetric fission products. This indicates complete relaxation of the relative velocity of the two fragments.

The approximately $1/\sin\theta_{\mathrm{c.m.}}$ shape of the fragment angular distributions in the emitter frame are displayed on Fig. 5 for the carbon target. Similar results are obtained for aluminum. One observes a systematic trend from backward peaked distributions for small values of M to forward peaked distributions for high M values, with a maximum asymmetry with respect to $\theta_{\mathrm{c.m.}} = 90°$ of about a factor 2. This may indicate that the lifetime of the system is of the order of magnitude of the time necessary for one rotation of the system (about 2×10^{-21} s), which is very long compared to fusion time (10^{-22} s, Ref. 34) and long compared to the equilibration time (5×10^{-22} s, Ref. 34). Thus, the intermediate mass fragments have the kinematical properties of an emission from an equilibrated composite system. The velocity integrated angular distributions present a bell-shaped behavior. Some of them are shown in Fig. 6.

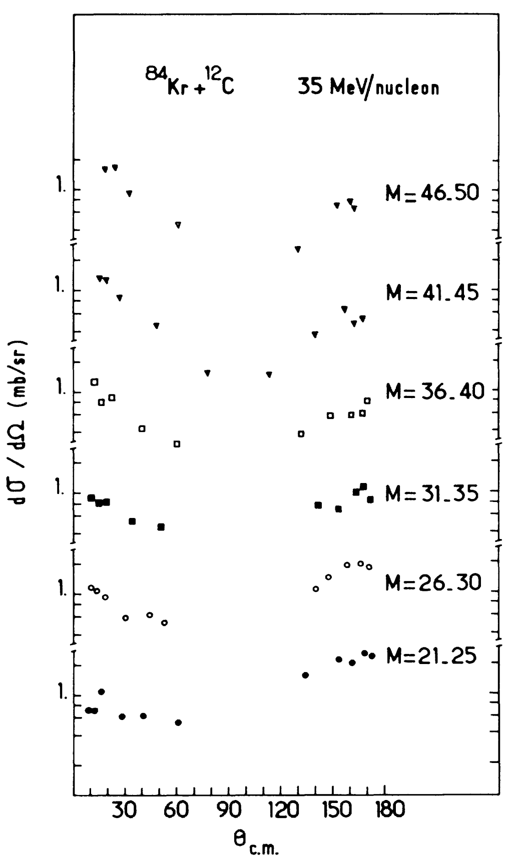

FIG. 5. Angular distributions in the emitter frame of heavy particles observed in the $^{84}Kr + ^{12}C$ reaction as a function of their masses integrated over five mass units.

The total cross sections are reported in Fig. 7 for both targets. The angular domain covered in the present experiment allowed us to obtain reliable values of the total cross section for the Z and M values shown in Fig. 7. For lower (higher) Z and M values larger (smaller) angles would have to be measured, as can be inferred from Fig. 6. Deeply "U-shaped" yields are found with cross sections about 1 order of magnitude higher for Al. A pronounced minimum is observed at $M \sim 35$. Assuming that the dominant emission process is the breakup of a composite system of mass M_{res} into two fragments, symmetry of the mass yield with respect to $M_{\mathrm{res}}/2$ is expected, $M_{\mathrm{res}} \sim 75$ (see Table I) is obtained for both targets. This value is in agreement with the results of the preceding kinematical analysis. Moreover, the minimum in the emission probability distribution shows that asymmetric splitting of M_{res} is favored.

The existence of well defined composite systems is confirmed by the coincident events, as can be seen in Fig. 8. The total mass $M_1 + M_2$ spectra show well defined peaks centered at 77 (FWHM = 8) and 71 (FWHM = 14) for carbon and aluminum, respectively, in good agreement with the previous results (see Table I). The preference for asymmetric mass splits, already observed in Fig. 7, is apparent from the figure.

In the two-body decay approximation, the velocity of the emitter can be reconstructed event by event by using the relationship

$$\mathbf{V}_{\mathrm{em}} = (M_1 \mathbf{V}_1 + M_2 \mathbf{V}_2)/(M_1 + M_2) .$$

The resulting scatter plots and spectra of the velocity components parallel ($V_{\parallel}$) and transverse ($V_{\perp}$) to the beam direction are reported in Fig. 9. In the carbon case the $V_{\parallel}$ distribution is centered around the velocity V_{CN} (CN denotes compound nucleus) expected for full momentum transfer and has the same width as the $V_{\perp}$ distribution. This confirms that essentially full momentum transfer precedes events that lead to heavy fragment emission. In contrast, for the aluminum target, the $V_{\parallel}$ distribution is centered between V_{CN} and the beam velocity, and the widths $\sigma_{\parallel}$ and $\sigma_{\perp}$ of the spectra $V_{\parallel}$ and $V_{\perp}$ are very different. This features shows a major contribution of incomplete fusion, in agreement with the analysis of the inclusive measurements. An estimation of the incomplete momentum transfer width σ_i can be obtained assuming that $\sigma_{\parallel}^2 = \sigma_{\perp}^2 + \sigma_i^2$. Using Fig. 9 and the above relation, one finds that the incomplete fusion process ranges from complete fusion to the absorption of about 10 mass units of the ^{27}Al target, supposing a linear relation between the linear momentum and the mass transfer.

Thus, all the experimental findings coherently indicate the formation of rather equilibrated emitters which break predominantly in two asymmetric fragments having a mean total residual mass of about 75 and a separation energy consistent with the low energy fission results. The excitation energy E^* of these emitters may be estimated using

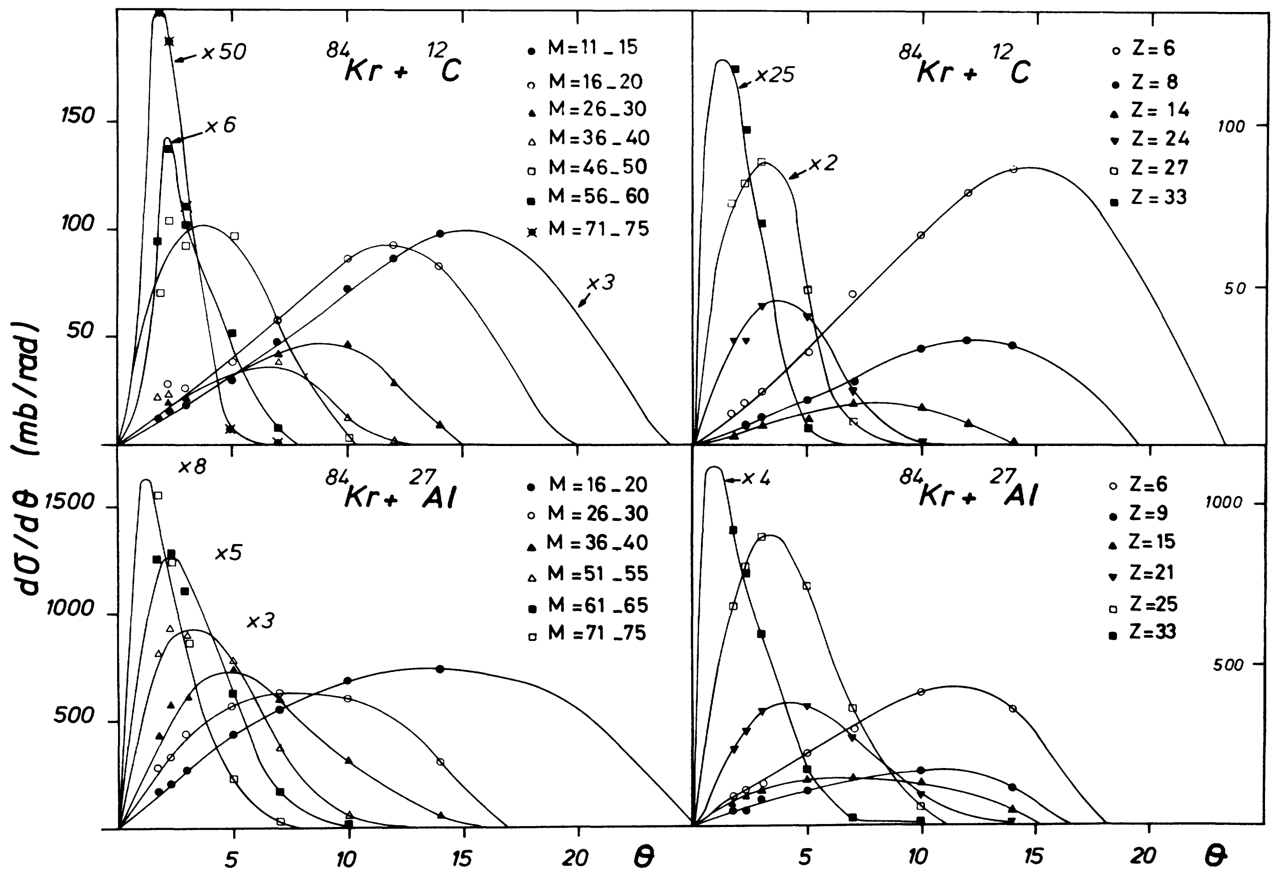

FIG. 6. Laboratory angular distributions of some products from both the ^{84}Kr+^{12}C and ^{84}Kr+^{27}Al collisions as a function of mass (left-hand side) and of atomic number (right-hand side). The symbols represent the experimental data, while the smooth curves have been used to extract the angle integrated cross section.

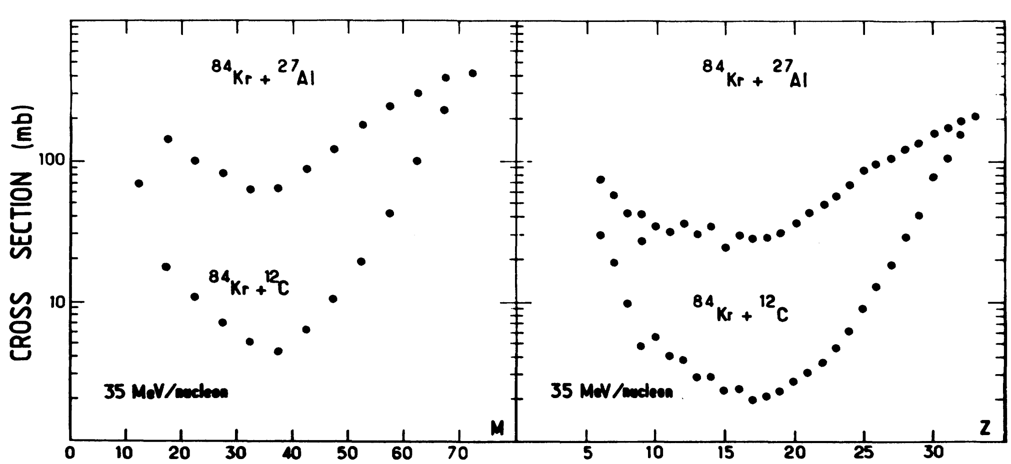

FIG. 7. Angle integrated cross sections as a function of ejectile mass for bins of five mass units (left) or as a function of atomic number (right).

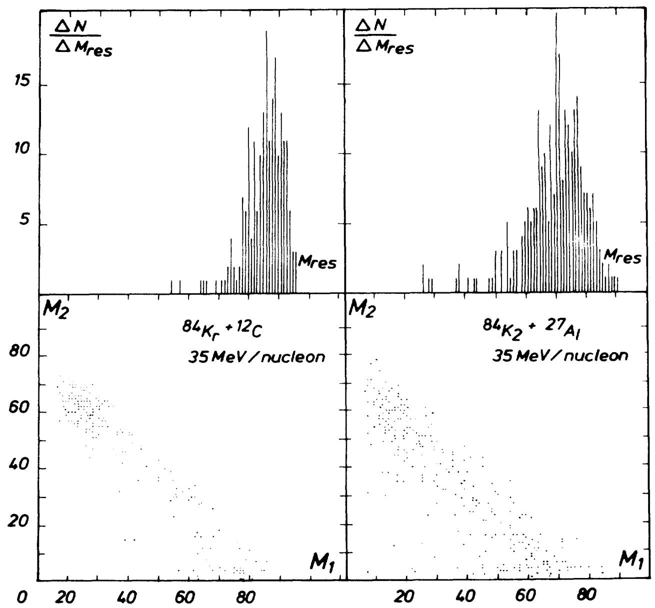

FIG. 8. Coincidences between the two time-of-flight telescopes. Lower part: scatter plots of the coincidence recorded in the present experiment for the carbon target (left-hand side) and for the aluminum target (right-hand side). Upper part: spectra of the sum of the masses, M_1+M_2, obtained from the corresponding scatter plots.

$$E^* = \Delta M \frac{84}{84+\Delta M} \times 35 \text{ MeV},$$

where ΔM is the absorbed fraction of the target taken equal to the fraction of linear momentum transferred. The values obtained in this way are reported in Table I and correspond to very high excitation energies. On this basis, we have tried to reproduce the data via statistical model calculations.

III. STATISTICAL MODEL FOR THE EMISSION OF HEAVY FRAGMENTS

Highly sophisticated and precise methods for the computation of statistical sequential decay by emission of light particles have been developed for moderate excitation energies.[19,20] However, the generalization of these codes to the emission of clusters of any size and excitation energy seemed very difficult. The method of Moretto[12] provides, as emphasized by Swiatecki,[13] a coherent description going from light particle emission to fission via the emission of heavy fragments. Thus it seemed very appropriate for the present case. It has been applied with success to the emission of heavy fragments in the mass region $M \sim 100$ at 70–100 MeV excitation energy.[21]

We have written a code (EDCATH) that follows this approach and, in addition, takes into account the angular momenta in the calculation of the branching ratio of different binary partitions. At each stage of the sequential

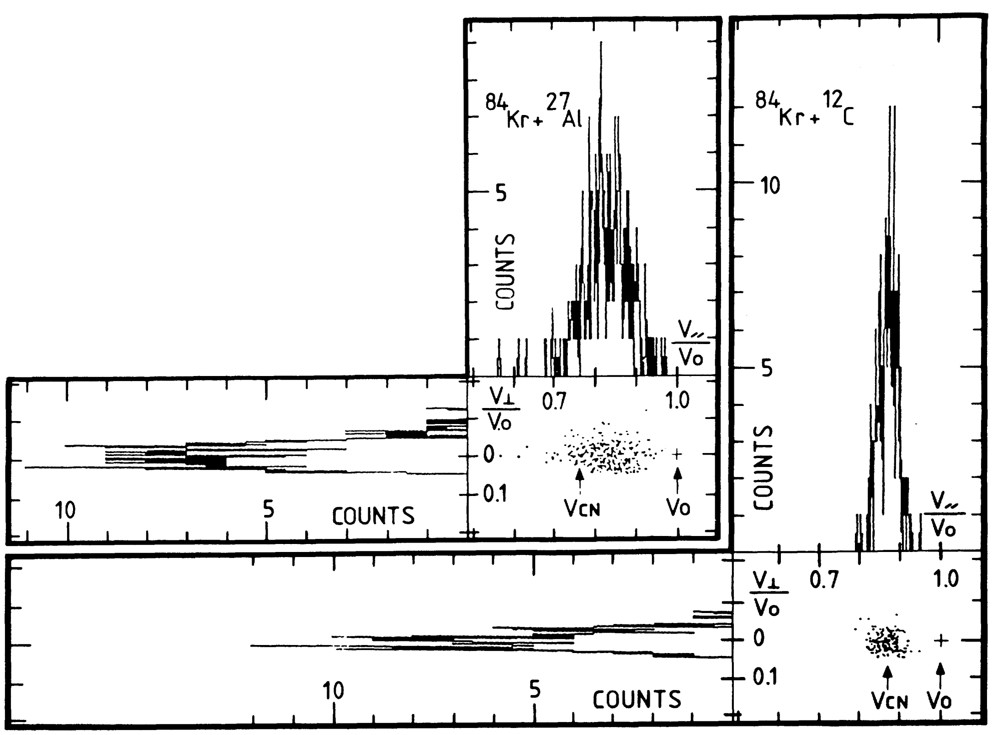

FIG. 9. Scatter plots of the velocity of the emitter obtained from coincidences by an event by event analysis (see text). $V_{\parallel}$ and $V_{\perp}$ are the velocities parallel and perpendicular to the beam direction. In the top and the left of the scatter plots the projections onto the $V_{\parallel}$ and the $V_{\perp}$ axes, respectively, are shown. The velocity V_{CN} for full momentum transfer and the beam velocity V_0 are also indicated.

cascade starting from an emitter characterized by a mass M, an atomic number Z, an excitation energy E^*, and an angular momentum l, the partial width is[12,13] proportional to the level density at the saddle point

$$\Gamma(M_1,Z_1,M_2,Z_2)=\frac{1}{2\pi}T(E^*/U)^2 \times\exp[2\sqrt{aU}-2(aE^*)^{1/2}]\ , \quad (3)$$

with

$$U=E^*+Q(M_1,Z_1,M_2,Z_2) -V_{\mathrm{SP}}(M_1,Z_1,M_2,Z_2)-E_{\mathrm{rot}}(l)\ . \quad (4)$$

The Q value for a given binary partition of M,Z into M_1,Z_1 and M_2,Z_2 is chosen to be the weighted mean from mass tables[22] (Q_{MT}) and liquid drop masses (Q_{LD}),

$$Q=Q_{\mathrm{MT}}X+Q_{\mathrm{LD}}(1-X)\ , \quad (5)$$

with

$$X=\exp(-a_qT)\ .$$

This dependence accounts for the disappearance of shell effects at high temperature T, which is defined as

$$U=aT^2-\tfrac{3}{2}T\ . \quad (6)$$

$a=M/(8.5\ \mathrm{MeV})$ is the level density parameter.

The liquid drop mass formula was taken from Ref. 23. This dependence on the shell effects was necessary to reproduce the transition from asymmetric fission at low excitation energy in actinidium nuclei to symmetric fission in the lead region. The parameter a_q was chosen equal to 1/MeV in order to correspond to the calculation of Ref. 24. For the saddle point energy V_{SP} we used ei-

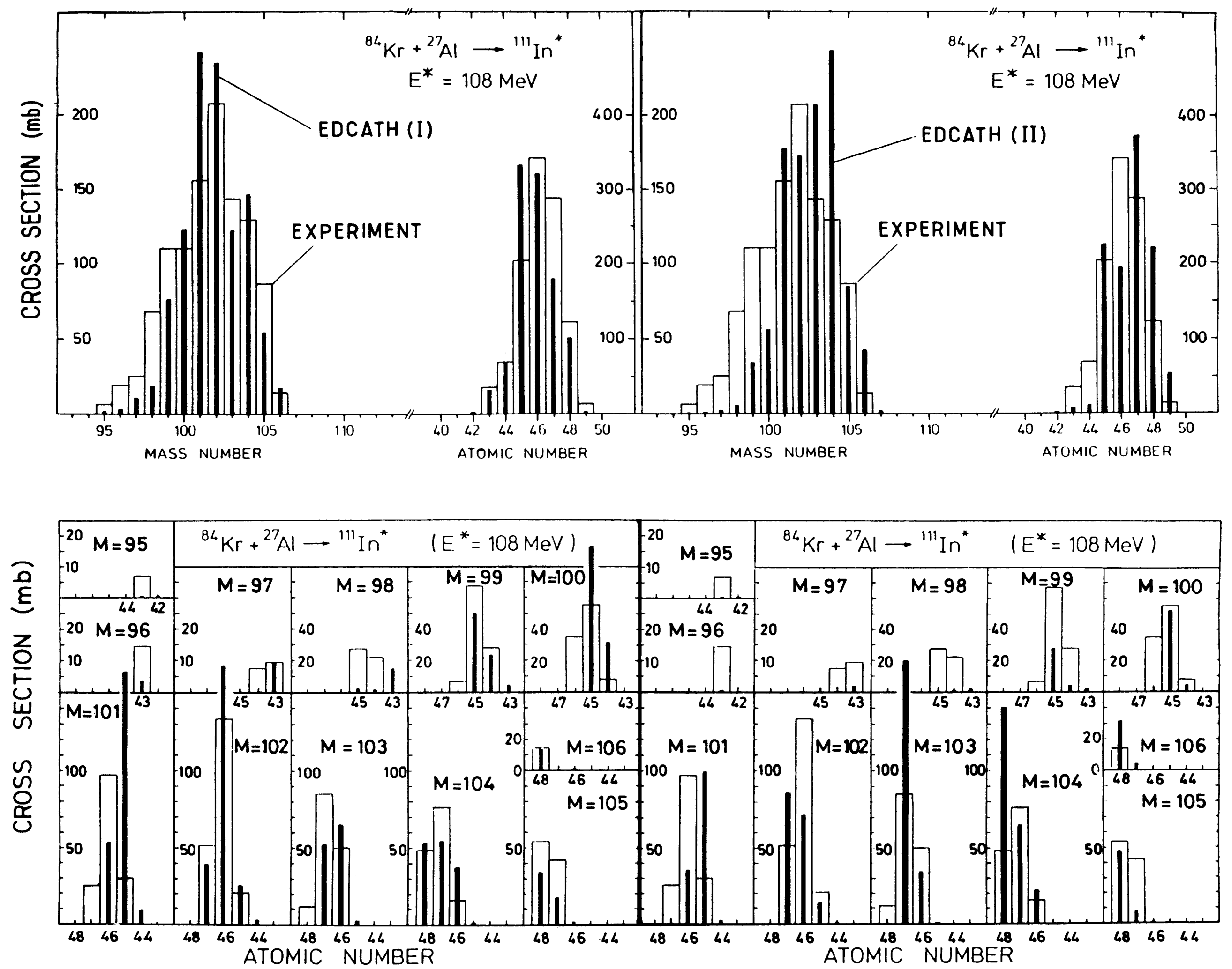

FIG. 10. Integrated cross section for the fusion-evaporated residues observed in the $^{84}Kr+^{27}Al$ reaction at 490 MeV incident energy (Ref. 26). Upper part: the experimental yields of Ref. 26 (histogram) as a function of mass and of atomic number are compared to the statistical calculation (black lines) (I) done using the potential of Viola (Ref. 18) on the left and using the potential of Krappe and Nix (Ref. 25) (II) on the right. Lower part: same as the upper part, but for isobaric yields.

ther the empirical formula of Viola[18] or the formulas of Ref. 25. The rotational energy $E_{\rm rot}(l)$ is calculated in the sticking limit, as well as the angular momenta and the rotational energies $E_{{\rm rot}_1}, E_{{\rm rot}_2}$ of the two fragments.

The available excitation energy E_f^* after separation of the fragments is distributed proportionally to their masses:

$$U_1 = M_1 E_f^* / M + E_{{\rm rot}_1} , \tag{7a}$$

$$U_2 = M_2 E_f^* / M + E_{{\rm rot}_2} , \tag{7b}$$

where

$$E_f^* = U - E_{{\rm rot}_1} - E_{{\rm rot}_2} - 2T .$$

The term $2T$ contains the mean kinetic energy[13] of a particle emitted at a temperature T.

It seems to us that there is presently some confusion about the distribution of the excitation energy on the fragments. Therefore we will try to clarify it and justify Eqs. (7) in the Appendix.

For the decay of the nucleus M,Z into M_1,Z_1 and M_2,Z_2 all combinations contained in the mass table are taken into account. The decay of heavy nuclei may go through very neutron rich nuclei not included in the mass table.[21] Thus the mass table is complemented by liquid drop masses[23] in the N/Z region of the initial nucleus.

At each separation, the preceding relations determine the excitation energy and the angular momentum of the fragments. Their decay is treated in the same way. To limit the calculation time, for a given initial angular momentum and for a fragment of a given M,Z, only the ten most probable paths are retained for further decay calculations. The calculation is pursued until complete cooling down of all fragments. Note that fluctuations are not treated in Eqs. (3)—(7); that is, distributions are replaced by mean values.

In order to verify the accuracy of the present approach, we compared the calculation to experimental results on the system ^{84}Kr+^{27}Al at $E^* = 108$ MeV, for which the yield of fusion-evaporation products and fusion-fission—like products have been measured.[26,27] The limiting angular momentum l_m for the population of the compound system in the sharp cutoff approximation was taken as $l = 68\hbar$ from Ref. 26. The comparison with the experimental mass and atomic number distributions[26] of fusion-evaporation residues is shown in Fig. 10. The good agreement implies that the number of evaporated light particles (p,n,α) is correctly predicted.

The results for fusion-fission—like events[27] are shown in Fig. 11. The agreement with the absolute value of the cross section shows that the competition of fission with evaporation is correctly treated, and the agreement with the width of the atomic number distribution demonstrates the correct evaluation of the saddle point energy [Eqs. (3)—(7)]. Calculation with the potential of Viola[18] and that of Ref. 25 gave qualitatively the same results (see Fig. 10), showing that the result is not too sensitive to small parameter changes.

The result of the calculation for the present ^{84}Kr+^{12}C experiment is shown in Fig. 12. An excitation energy corresponding to complete fusion has been taken. The predictions are not very sensitive to this parameter within a

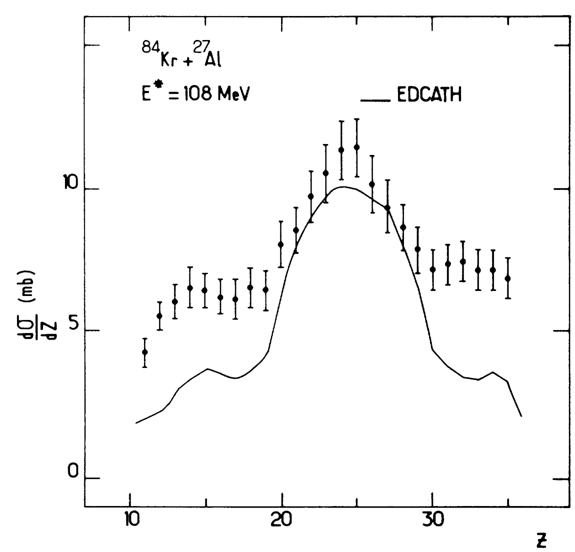

FIG. 11. Experimental cross section from Ref. 27 for the fusion-fission—like residues as a function of the atomic number are compared to the solid line representing the theoretical prediction (see text).

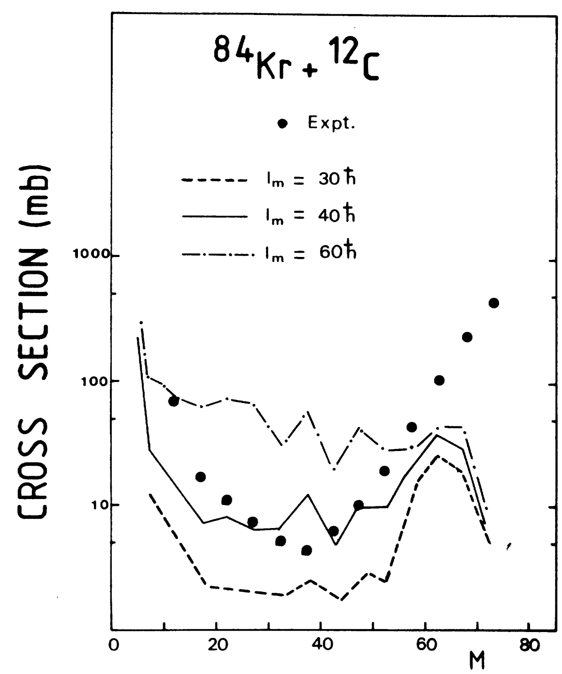

FIG. 12. Angle integrated cross section as a function of mass, for mass bins of 5, in the ^{84}Kr+^{12}C reaction at $E = 35$ MeV/nucleon. The dots represent the experimental data and the lines indicate statistical model calculations for different values of l_m.

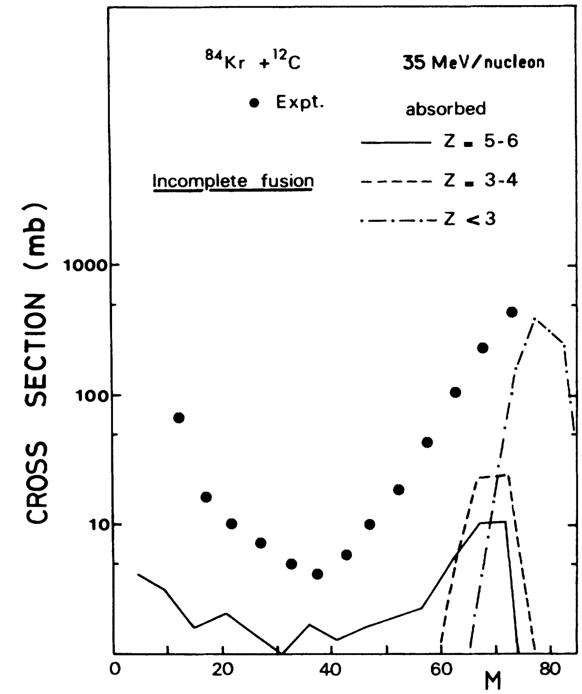

FIG. 13. Statistical model prediction for incomplete fusion (Ref. 28). The lines show the calculated yields for different absorbed parts of the target; otherwise, same as Fig. 12.

variation of about 10%, which is the uncertainty indicated in the experimental momentum transfer evaluation (see Table I). The maximum l value in the sharp cutoff approximation was varied as shown in Fig. 12 and it was found that $l_m = 30\hbar$ leads to a U-shaped mass distribution. Starting from high cross-section values for light elements, it gradually flattens in the symmetric fission region and is ended by the heavy residue evaporation peak centered at $M \sim 65$. The predicted cross section is too small.

The shape of the absolute value of the mass distribution are in disagreement with data for $l_m = 60\hbar$. The filling of the valley of intermediate mass residues reveals an overly strong enhancement of the symmetric fission process, which is due to the high angular momenta allowed. Good agreement is obtained in the 20–60 mass range when using $l_m = 40\hbar$. This angular momentum is nearly equal to the value tabulated by Wilcke *et al.*,[16] which is the critical angular momentum l_{crit} for complete fusion in the formulation of Wilczynski *et al.*,[28] including rolling as proposed by Bass.[29]

Geometrically, this l_m value corresponds to the upper limit of the impact parameter for which the ^{12}C completely overlaps with the ^{84}Kr. Up to this limit for this asymmetric system, an abrasion model[30] also predicts complete absorption of the ^{12}C by the ^{84}Kr. In this model the kinetic energy of the participant nucleons in the interaction region is not high enough to allow its abrasion.

The disagreement observed for masses greater than 60 may be due to incomplete fusion reactions, which are expected to play an important role at the present energy. Thus, following the formulation of Ref. 28 in the rolling limit, we took into account the incomplete fusion of ^{12}C with ^{84}Kr. The bin-model approximation[31] was adopted for the sake of simplicity. In this picture the increase in the entrance channel of the angular momentum above l_{crit} leads to higher composite systems with smaller total angular momenta and lower excitation energies. At the beam energy considered here, the lighter the mass of the composite system, the higher the mass of the residues after statistical decay, as shown in Fig. 13. As expected, the in-

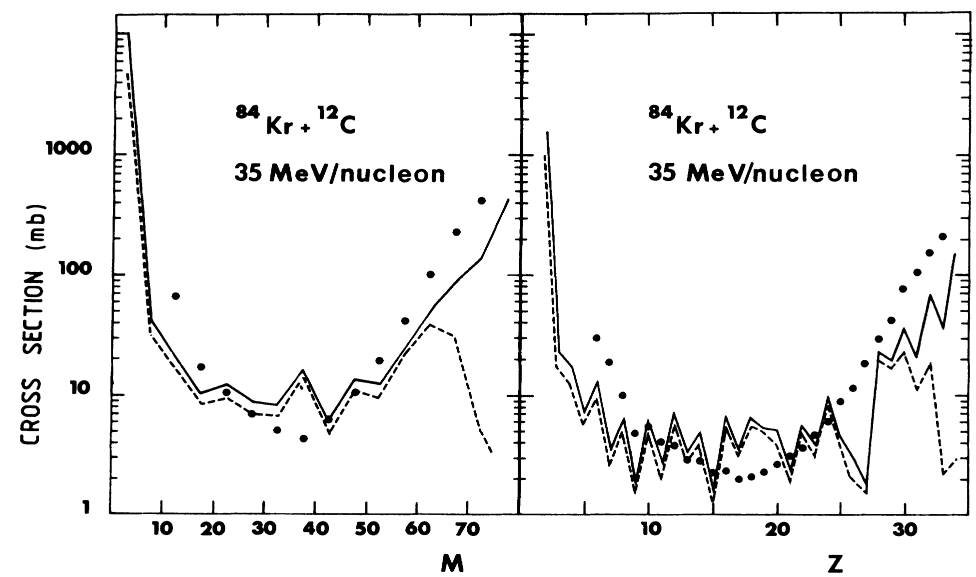

FIG. 14. Total yields as a function of mass and of atomic number predicted by the statistical model compared to the experimental data. The dashed line represents the complete fusion contribution and the solid line shows the sum of complete and incomplete fusion.

complete fusion contributes significantly for masses greater than 60 only. The sum of incomplete and complete fusion reproduces the data well (Fig. 14). The staggering of the predicted yields may be attributed to the fact that no fluctuations have been included in the calculation, as pointed out before. The complete and incomplete fusion represent 10% and 30% of the total cross section, respectively. The predicted mass correlation of heavy nuclei emitted in coincidence agrees also with the data (see Fig. 15).

When considering the $^{84}Kr+^{27}Al$ system, the incomplete fusion model of Wilczynski et al.[28] in the presently used parametrization was not able to describe the production of intermediate mass nuclei. In this model there is essentially either more or less complete fusion, which leads to explosion of the composite system or very incomplete fusion that does not excite the composite system sufficiently. We therefore apply a geometrical overlap model, assuming that the nucleons of the lighter partner in the overlap region are absorbed and thermalized by the heavy partner, as predicted by a more refined version of Dayras et al.[30] Then, there is a direct relation between the impact parameter, the mass transfer, the angular momentum, and the excitation energy of the composite system. The angular momentum and the transferred mass as a function of the impact parameter is shown in Fig. 16 for both systems. The formation cross section of an impact parameter b is proportional to $2\pi b\,db$. This model gives about the same results as the Wilczynski model for the $^{84}Kr + ^{12}C$ data (see Fig. 17).

The 1 order of magnitude increase of the cross section for the $^{84}Kr+^{27}Al$ data is correctly reproduced for $M \leq 45$. The mean momentum transfer as a function of the detected mass is correctly reproduced in this model, including the striking difference of the behavior of the two systems (upper part of Fig. 4). However, the experimental increase of the cross section for $M \geq 45$ is not reproduced. Considering the mass region $M = 60-65$, one may infer from Fig. 3(b) that two components exists in the velocity spectra. Contrary to what would be expected for a single component, the width of the velocity spectrum decreases with increasing angle, together with a displacement of the maximum to lower values of V/V_0. This indicates that here a strongly relaxed component is

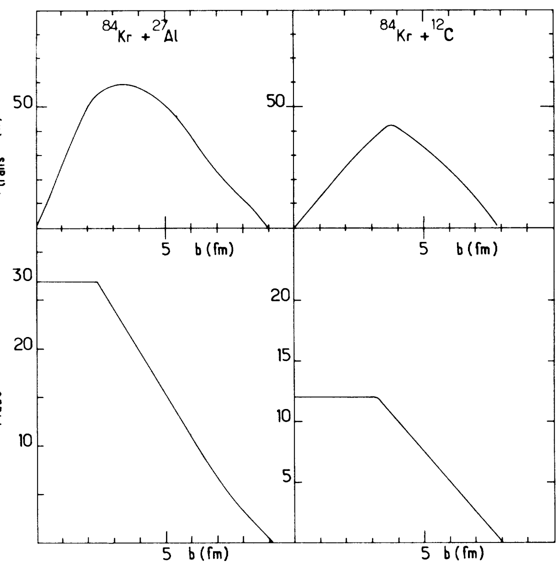

FIG. 16. Transferred angular momentum and absorbed mass as a function of the impact parameter b, calculated using a geometrical abrasion-absorption model (see text).

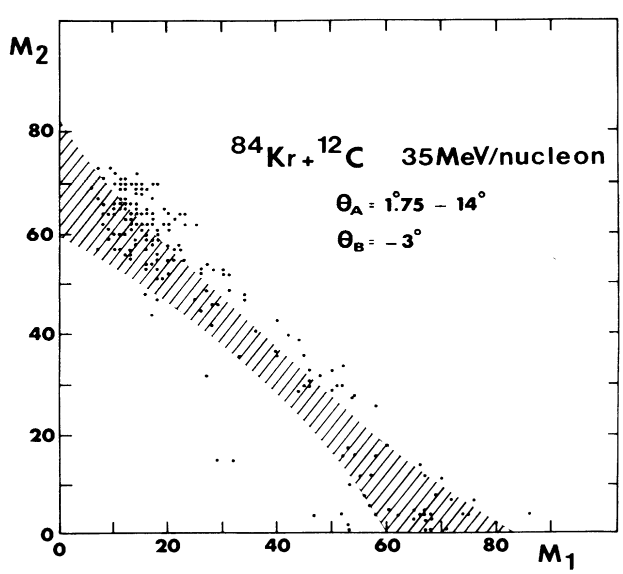

FIG. 15. Statistical model calculation (shaded region) for complete and incomplete fusion compared to the experimental mass correlation (points) of Fig. 8.

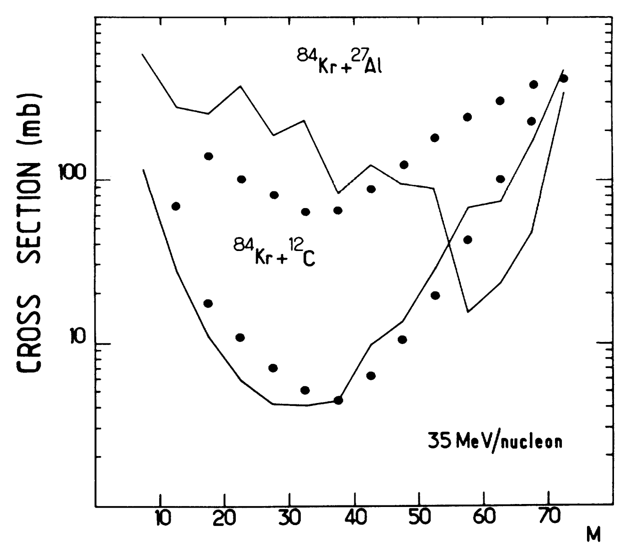

FIG. 17. Total yields vs mass as obtained from the statistical model using the geometrical abrasion-absorption description for complete and incomplete fusion of Fig. 16. Otherwise, same as in Fig. 7.

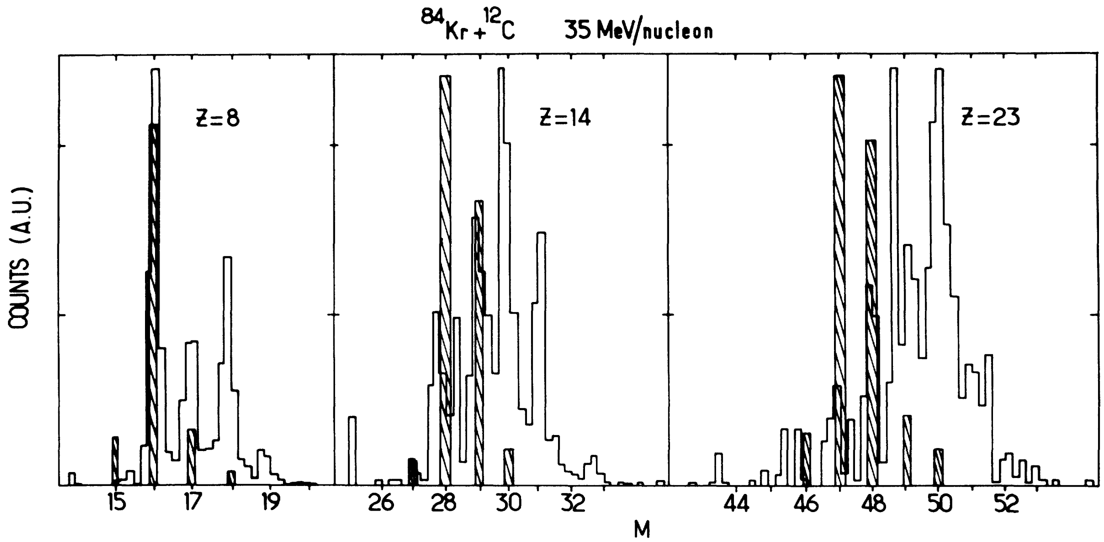

FIG. 18. Histograms of experimental isotopic distributions, compared to calculations based on the statistical model with abrasion-absorption processes in the entrance channel (Fig. 16).

mixed with a quasielastic component. A tentative decomposition allows one to attribute less than 30% of the yield to the relaxed component. The quasielastic component should be due to the projectile fragmentation. In the model used here, only the abrasion-incomplete fusion of the light partner (Al) is taken into account, whereas abrasion of the Kr and transfer from Kr to Al are not treated. Such an asymmetry of the treatment is a defect of all present abrasion-incomplete fusion models,[30,32] to our knowledge, and the observed discrepancy could originate from this defect of the entrance channel model. More detailed studies of this effect, involving heavier targets and other beam energies, are actually in progress.

Another point to be investigated is the influence of the very short lifetime at high excitation energy. This may not favor the emission of very heavy fragments because of the relatively long time necessary for such a process.[33] Some indication of such an influence may be present in the mass distributions of individual atomic numbers (Fig. 18). The model predicts less neutron rich isotopes than observed experimentally. This may indicate the influence of some nonequilibrium process. Nevertheless, a preequilibrium model calculation[34] predicts a linear momentum transfer and excitation energies that are close to the values given in Table I.

IV. CONCLUSION

Experimental results on the systems $^{84}Kr+^{12}C$ and $^{84}Kr+^{27}Al$ at 35 MeV/nucleon have been presented. For the Kr + C system a kinematical analysis of the intermediate mass fragments ($M=15$–40), which represent about 10% of the total cross section, shows that these products are emitted by a composite system having all the characteristics of total thermalization, i.e., $(95\pm10)\%$ of linear momentum transfer and 357 ± 40 MeV excitation energy. The same analysis for the Kr + Al system leads to $(80\pm10)\%$ linear transfer and 600 ± 60 MeV excitation energy. This last value approaches the limit of stability predicted by theory,[4] as shown in Fig. 19. Even if the value of the excitation energies is model dependent, we think that the values in the present case are reliable, as is shown by the good overall agreement of the model calcu-

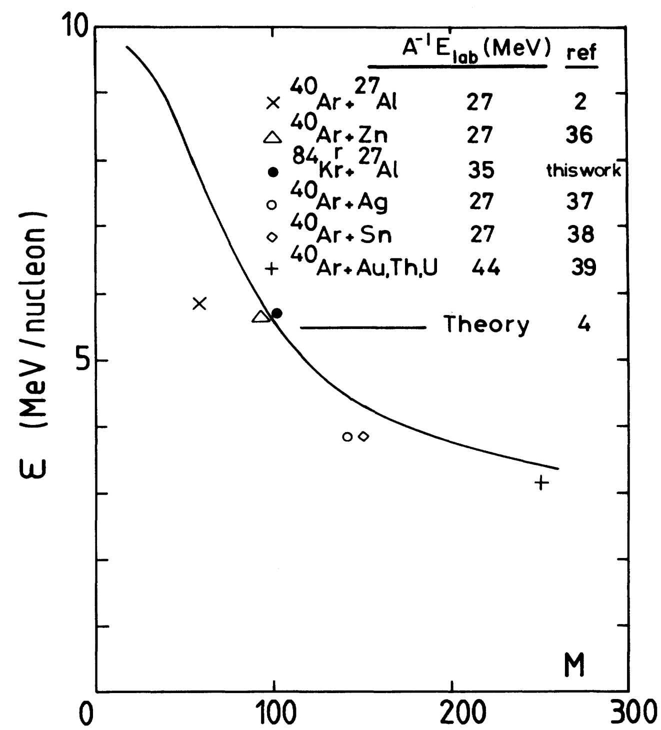

FIG. 19. Excitation energy per nucleon as a function of the mass of the composite nucleus. The curve represents the theoretical prediction of Ref. 4. Note that this prediction is quite parameter dependent (Ref. 4). Included on this figure are some results from other works.

lation with the data. Such high excitation energies seemed impossible some years ago. Coincidence measurements confirmed the binary character of the fragment emission.

A statistical model calculation of evaporation of hot fragments following complete and incomplete fusion agrees well with the Kr + C data. The increase by 1 order of magnitude of the cross sections for $^{84}Kr+^{27}Al$ was well reproduced for $M \leq 45$. However, the yield for masses $M \geq 45$ was mismatched, probably indicating an inadequacy of the incomplete fusion models used. Experimental data on heavy fragments thus appears to comprise a sensitive test of these models.

APPENDIX

We consider the level density of a nucleus of A nucleons at an excitation energy U and compare it to the level density of two separated subsystems of A_1 and A_2 nucleons at an excitation energy U_1 and U_2, respectively. The rotational energy and the angular momentum do not modify the argumentation and will be omitted.

The total level density of the subsystems is

$$\frac{\partial^2 n}{\partial U_1 \partial U_2} = \rho_1(A_1, U_1)\rho_2(A_2, U_2) \ . \tag{A1}$$

The level density at a given total excitation energy $U = U_1 + U_2$ is

$$\rho_{12}(A,U) = \int \rho_1(A_1,U_1)\rho_2(A_2, U-U_1)dU_1 \ . \tag{A2}$$

Using for ρ the expression of Ref. 35,

$$\rho(A,U) = \frac{1}{\sqrt{48}}\frac{1}{U}\exp(2\sqrt{AU}) \ , \tag{A3}$$

one obtains

$$\rho_{12}(A,U) = \frac{1}{48}\int \frac{1}{U_1}\frac{1}{U-U_1} \times \exp[2\sqrt{a_1 U_1} + 2\sqrt{a_2(U-U_1)}]dU_1 \ . \tag{A4}$$

At high excitation energy the dependence of the integrand on U_1 is dominated by the exponential function. The maximum of this function, U_{10}, is given by

$$\frac{a_1}{\sqrt{a_1 U_{10}}} - \frac{a_2}{\sqrt{a_1(U-U_{10})}} = 0 \ . \tag{A5}$$

Using $a_1 = A_1/a_s$ and $a_2 = A_2/a_s$, one immediately gets

$$\frac{U_{10}}{A_1} = \frac{U_{20}}{A_2} = \epsilon_0^* \ , \tag{A6}$$

which means that the maximum of the total level density corresponds to the same excitation energy per nucleon for both fragments. This result is obtained without any assumption on thermal equilibrium between the two subsystems. $U = aT^2$ and (A6) gives the equality of the temperature $T_1 = T_2$.

The argument of the exponential function can be expanded up to second order around the maximum and the analytical integration over U_1 is possible, with the result

$$\rho_{12}(U) = \frac{1}{48}\left[\frac{A_1 + A_2}{A_1 A_2}\right]^{1/2}\left[\frac{a_s}{\epsilon_0^*}\right]^{1/4}\frac{1}{U}\exp(2\sqrt{aU}) \ , \tag{A7}$$

where the relations $U = aT^2$ and $a = A/a_s$ have been used.

The dependence of Eqs. (A7) and (A3) on the total excitation energy U is identical. However, the factor in front is somewhat different. This means that the level density of the combined subsystems is not the same as that of a unique system having the same total mass. In principle, there should be a continuous evolution from (A3) to (A7) summed over all combinations A_1 and A_2 during the evolution of the composite system to scission. Such an evolution could be introduced in the method by a shape dependent level density parameter a_s.[40]

---

[1] D. Jacquet, E. Duek, J. M. Alexander, B. Borderie, J. Galin, D. Gardès, D. Guerreau, M. Lefort, M. Monnet, M. F. Rivet, and X. Tarrago, Phys. Rev. Lett. **53**, 2226 (1984).

[2] G. Auger, D. Jouan, E. Plagnol, F. Pougheon, F. Naulin, H. Doubre, and C. Grégoire, Z. Phys. A **321**, 243 (1985); in Proceedings of the International Winter Meeting on Nuclear Physics, Bormio, Italy, 1985.

[3] W. Mittig, A. Cunsolo, A. Foti, J. P. Wieleczko, F. Auger, B. Berthier, J. N. Pascaud, J. Québert, and E. Plagnol, Phys. Lett. **154B**, 259 (1985).

[4] P. Bonche, S. Levit, and D. Vautherin, Nucl. Phys. **A427**, 278 (1984).

[5] D. R. Decan and U. Mosel, in Proceedings of the International Winter Meeting on Nuclear Physics, Italy 1985, p. 798.

[6] J. P. Bondorf, Nucl. Phys. **A387**, 25 (1982).

[7] A. D. Panagiotou *et al.*, Phys. Rev. Lett. **52**, 496 (1984).

[8] H. H. Heckman, D. E. Greiner, P. J. Lindstrom, and H. Shwe, Phys. Rev. C **17**, 1735 (1978).

[9] V. Borrel, D. Guerreau, J. Galin, B. Gatty, D. Jacquet, and X. Tarrago, Z. Phys. A **314**, 191 (1983).

[10] J. Barrette, B. Berthier, E. Chavez, R. Dayras, H. Delagrange, B. Heusch, G. Lanzano, R. Legrain, M. Mermaz, W. Mittig, A. Pagano, A. Palmeri, and E. Pollaco, in Proceedings of the XXIInd International Meeting on Nuclear Physics, Bormio (Italy), 1984, p. 561.

[11] J. B. Natowitz, N. M. Namboodiri, and E. T. Chulik, Phys. Rev. C **13**, 171 (1976).

[12] L. Moretto, Nucl. Phys. **A247**, 211 (1975).

[13] W. J. Swiatecki, Lawrence Berkeley Laboratory Report No. LBL 11403, 1983.

[14]F. Auger, B. Berthier, A. Cunsolo, A. Foti, W. Mittig, J. M. Pascaud, E. Plagnol, J. Québert, and J. P. Wieleczko, in Proceedings of the XXIIIrd International Winter Meeting on Nuclear Physics, Bormio, Italy, 1985.
[15]F. Auger, B. Berthier, A. Cunsolo, A. Foti, W. Mittig, J. M. Pascaud, E. Plagnol, J. Québert, and J. P. Wieleczko, in Proceedings of the 4th International Conference Nuclear Reaction Mechanisms, Varenna, Italy, 1985.
[16]W. W. Wilcke, J. R. Birkelund, H. J. Wollersheim, A. D. Hoover, J. R. Huizenga, W. U. Schröder, and L. E. Tubbs, At. Data Nucl. Data Tables **25**, 389 (1980).
[17]V. E. Viola, Jr. *et al.*, Phys. Rev. C **26**, 178 (1982).
[18]V. E. Viola, Jr., Nucl. Data Sect. A **1**, 391 (1966).
[19]J. Gomez Del Campo, Phys. Rev. C **19**, 2170 (1979).
[20]F. Pühlhofer, CASCADE, a Nuclear Evaporation Code, Internal Report, GSI, Darmstadt, 1979.
[21]L. G. Sobotka, M. L. Padgett, G. J. Wozniak, G. Guarino, A. J. Pacheco, L. G. Moretto, Y. Chan, R. G. Stokstad, I. Tserruya, and S. Wald, Phys. Rev. Lett. **51**, 2187 (1983).
[22]A. H. Wapstra and K. Bos, At. Data Nucl. Data Tables **19**, 177 (1977).
[23]P. A. Seeger and R. C. Perisho, Los Alamos Scientific Laboratory Report No. LA-3751, 1967; see also Ref. 24.
[24]B. D. Wilkins, E. P. Steinberg, and R. R. Chasman, Phys. Rev. C **14**, 1832 (1976).
[25]H. J. Krappe, J. R. Nix, and A. J. Sierk, Phys. Rev. C **20**, 992 (1979).
[26]W. F. W. Schneider, F. Pühlhofer, R. P. Chestnut, C. Volant, H. Freisleben, W. Pfeffer, and B. Kohlmeyer, Nucl. Phys. **A371**, 493 (1981).
[27]B. Heusch, H. Freisleben, W. F. W. Schneider, B. Kohlmeyer, H. Stege, and F. Pühlhofer, Z. Phys. A **332**, 309 (1985).
[28]J. Wilczynski, K. Siwek-Wilczynska, J. Van Driel, S. Gonggrijp, D. C. J. M. Hageman, R. V. F. Janssens, J. Lukasiak, R. H. Siemssen, and S. Y. Van Der Werf, Nucl. Phys. **A373**, 109 (1982).
[29]R. Bass, Nucl. Phys. **A231**, 45 (1974).
[30]R. Dayras *et al.*, Nucl. Phys. (to be published).
[31]J. Wilczynski, K. Siwek-Wilczynska, J. Van Driel, S. Gonggrijp, D. C. J. M. Hageman, R. V. F. Janssens, J. Lukasiak, and R. H. Siemens, Phys. Rev. Lett. **45**, 606 (1980).
[32]B. G. Harvey and H. Homeyer, Lawrence Berkeley Laboratory Report No. LBL 16882, 1983.
[33]H. Delagrange, C. Grégoire, F. Scheuter, and Y. Abe, GANIL report, p. 85-07, 1985.
[34]M. Blann, Phys. Rev. C **31**, 1245 (1984).
[35]A. Bohr and B. R. Mottelson, *Nuclear Structure* (Benjamin, Reading, Mass., 1985), Vol. I.
[36]F. Rami, J. P. Coffin, G. Guillaume, B. Heusch, P. Wagner, A. Fahli, and P. Fintz, Nucl. Phys. **A444**, 325 (1985).
[37]B. Borderie and M. F. Rivet, Z. Phys. A **316**, 243 (1984).
[38]J. Blachot, J. Crançon, B. de Goncourt, A. Gizon, and A. Lhères, Z. Phys. A **321**, 645 (1985).
[39]M. Conjeaud, S. Harar, M. Mostefai, E. C. Pollaco, C. Volant, Y. Cassagnou, R. Dayras, R. Legrain, H. Oeschler, and F. Saint-Laurent, Phys. Lett. **159B**, 244 (1985).
[40]R. Balian and C. Bloch, Ann. Phys. (N.Y.) **60**, 401 (1970).